Supplement of Atmos. Chem. Phys., 22, 9033–9057, 2022
https://doi.org/10.5194/acp-22-9033-2022-supplement
© Author(s) 2022. CC BY 4.0 License.

Atmospheric Chemistry and Physics
Open Access

Supplement of

Particle phase-state variability in the North Atlantic free troposphere during summertime is determined by atmospheric transport patterns and sources

Zezhen Cheng et al.

Correspondence to: Swarup China (swarup.china@pnnl.gov)

The copyright of individual parts of the supplement might differ from the article licence.

S1. CCSEM-EDX Atomic Percentage Correction

EDX analysis of light elements such as C, N, and O is considered semi-quantitative, and C and O contributions from the B-film substrate. Therefore, we performed post-correction on the elemental percentage of C, N, and O. To do this, we used CNQX disodium salt (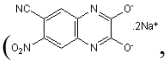 , CAS Number: 479347-85-8) as standard material, which has advantages such as 1) containing C, N, and O; 2) contain Na, which EDX can quantitatively analyze; 3) CNQX disodium salt is stable under the electrical beam; 4) CNQX disodium salt is soluble in the water so that we can generate CNQX disodium salt particles by nebulizing 0.5 g L^{-1} solution; 5) shape of CNQX disodium salt particle is spheric (see Fig. S1). Therefore, we performed CCSEM-EDX analysis on CNQX disodium salt particles and retrieved the following correction function for C, N, and O:

$$\mathrm{C_{real}} = (123.2 \pm 1.4) - (4.738 \pm 0.214)\log(\mathrm{H}) - (1.186 \pm 0.02)\mathrm{C_{measured}}, \mathrm{R^2} = 0.8484, \quad \text{(S1)}$$

$$\mathrm{O_{real}} = (13.68 \pm 0.18) - (0.3413 \pm 0.0636)\log(\mathrm{H}) + (0.2579 \pm 0.0072)\mathrm{O_{measured}}, \mathrm{R^2} = 0.937, \quad \text{(S2)}$$

$$\mathrm{N_{real}} = (1.101 \pm 0.002)\mathrm{N_{measured}}, \mathrm{R^2} = 0.791, \quad \text{(S3)}$$

Where $C_{measured}$, $N_{measured}$, and $O_{measured}$ are measured atomic percentages of C, N, and O, respectively, C_{real}, N_{real}, and O_{real} are expected atomic percentages of C, N, and O, respectively, which are calculated based on the stoichiometric ratio between that element and Na, and H is the hight of the particle (μm). Since the particles are spheric, the measured area equivalent diameter (μm) is approximately equal to the height of the particles. Therefore, when applying the correction function to our CCSEM-EDX data, we need to estimate the H by dividing the longest diameter retrieved from the CCSEM-EDX measurement by the aspect ratio retrieved from tilted images (see Sect. 3.3.2). Moreover, we only perform this correction when $C_{measured}$, $O_{measured}$, and $N_{measured}$ are not equal to 0 or 100% since these cases are not realistic. Furthermore, if corrected C, N, and O values are less than 0 or greater than 100%, we discard these data since they are also not realistic. Therefore, we applied this correction to measured C, N, and O, and after correction, we re-normalized the fraction of all elements. It should be kept in mind that this correction method is based on empirical fittings with assumptions that CNQX disodium salt particles are perfect spheric, and all particles have the same aspect ratio. The first assumption might lead to overestimating the particle height of CNQX disodium salt particles, and the second one might misrepresent the particle shape. Moreover, using one standard might not fully represent the chemical complexity of ambient particles. Thus, more data from different standards are necessary for improving this method.

S2. Glass transition temperature prediction

A range of glass transition temperature ($T_{g,org}$) for organic aerosols from June to July 2017 as a function of relative humidity (RH) has been estimated following the methods introduced by (Wang et al., 2012):

$$T_{\mathrm{g,org}}(\mathrm{RH}) = \frac{T_{\mathrm{g,w}}k_{\mathrm{GT}} + f(\mathrm{RH})T_{\mathrm{g,org}}(\mathrm{RH}=0\%)}{k_{\mathrm{GT}} + f(\mathrm{RH})}, \quad \text{(S4)}$$

where

$$f(\mathrm{RH}) = \frac{100-\mathrm{RH}}{\mathrm{RH}} \frac{1}{\kappa_{\mathrm{org}}} \frac{\rho_{\mathrm{org}}}{\rho_{\mathrm{w}}}, \quad \text{(S5)}$$

where $T_{g,w}$ is the T_g for pure water, k_{GT} is the Gordon-Taylor constant, κ_{org} is the CCN-derived hygroscopicity parameter of the organic fraction, ρ_{org} and ρ_w are the density of water and organic material, respectively. In this study,

we cannot retrieve T_g(RH = 0%) for particles. Therefore, we adopted previously reported values for these parameters, which were also retrieved at the Pico Mountain Observatory but on 27–28 June 2013, 5–6 July 2014, and 20–21 June 2015 (Schum et al., 2018). However, the T_g(RH = 0%) of these sampling periods is very stable (Schum et al. 2018). Therefore, we used the average value of T_g(RH = 0%) reported by (Schum et al., 2018) (332.09 K) to predict the T_g of particles in this study, and the highest and lowest value of T_g(RH = 0%) reported by Schum et al., 2018 (360.65K and 313.46K, respectively) as upper and lower bound. Moreover, k_{GT}, $T_{g,w}$, κ_{org}, and ρ_{org} were assumed to be 2.5 (Shiraiwa et al., 2017), 136 K (Kohl et al., 2005), 0.12 (Schum et al., 2018), and 1.4 g cm^{-3} (Schum et al., 2018), respectively.

Table S1. Additional information of Pico 2014 and Pico 2015 samples. Samples were collected at stage 3 (cut-off size: >0.15 μm) and/or stage 4 (cut-off size: >0.05 μm) of an MPS-4G1impactor

Sample ID	SA1	SA2	SA3	S1	S2	S3	S4	S5	S6
Date	04/07/2014	10/07/2014	12/07/2014	20/06/2015	26/06/2015	03/07/2015	10/07/2015	19/07/2015	26/07/2015
Time started	15:49	17:24	15:07	15:15	15:22	15:20	17:10	13:38	8:30
Time ended	21:00	20:22	18:33	15:50	17:58	19:09	18:40	17:51	15:00
Sampling stage	3	3	3	3 & 4	3 & 4	3 & 4	3 & 4	3 & 4	3 & 4
Average aging time (days)	16.4	16.2	16.0	15.7	12.2	10.5	12.3	16.1	17.1
# of STXM-NEXAFS analyzed particle	653	208	425	NA	NA	86	NA	37	NA
OC	5.4%	7.7%	8.7%	NA	NA	68.6%	NA	21.6%	NA
OCIN	82.7%	20.4%	76.9%	NA	NA	3.5%	NA	35.1%	NA
OCEC	2.0%	2.5%	0.5%	NA	NA	24.4%	NA	5.4%	NA
OCECIN	10.0%	6.6%	13.9%	NA	NA	3.5%	NA	37.8%	NA
Temperature measured at OMP (K)	NA	NA	NA	285.5±0.1	287.2±0.5	281.0±0.3	283.4±0.1	283.8±0.2	284.4±0.3
RH at OMP (%)	NA	NA	NA	47.8±1.7	61.3±2.4	67.3±2.3	26.2±0.8	NA	56.3±4.5

50

Table S2. Additional information of Pico 2017 samples. S3 and S4 mean samples were collected at stage 3 (cut-off size: >0.15 μm) and stage 4 (cut-off size: >0.05 μm) of an MPS-4G1impactor, respectively. The number inside the brackets represents the range of uncertainties.

Sample ID	S3-1	S3-2	S3-3	S3-4	S4-1	S4-2	S4-3	S4-4
Date	24/06/ 2017	27/06/ 2017	27/06/ 2017	29/06/ 2017	06/07/ 2017	09/07/ 2017	27/07/ 2017	29/07/ 2017
Time started	15:23	14:00	16:45	14:30	13:40	12:51	14:04	11:39
Time ended	17:23	14:22	17:15	15:00	14:20	14:01	14:14	11:51
Sampling stage	3	3	3	3	4	4	4	4
# of CCSEM-EDX Analyzed Particles	726	968	2573	1943	753	984	1503	592
OC (%)	6.3	6.7	14.1	4.2	16.6	13.5	2.4	9.8
CNO (%)	23.4	62.2	39.6	55.2	27.0	35.2	43.7	32.1
CNOS (%)	0.1	0.1	0.0	0.0	0.1	0.1	0.7	0.5
Sea salt (%)	28.2	8.9	28.0	11.3	19.4	28.9	24.8	31.6
sea salt/S (%)	31.5	17.6	14.1	27.4	5.2	13.3	22.8	13.5
Dust (%)	1.1	1.1	0.7	0.6	0.3	0.1	0.2	0.3
Sulfate coated dust (%)	0.1	0.1	0.1	0.0	0.1	0.0	0.2	0.2
Others (%)	9.1	3.3	3.5	1.4	31.3	8.9	5.2	12.0
# of STXM-NEXAFS analyzed particle	NA	NA	140	NA	NA	166	NA	NA
OC (%)	NA	NA	6.4	NA	1.2	NA	NA	NA
OCIN (%)	NA	NA	86.4	NA	98.8	NA	NA	NA
OCEC (%)	NA	NA	0.0	NA	0.0	NA	NA	NA
OCECIN (%)	NA	NA	7.1	NA	0.0	NA	NA	NA
Temperature measured at OMP (K)	NA	NA	285.1±0.2	286.8±0.2	287.7±0.3	284.9±0.3	291.90	285.8±0.1
Temperature from FLEXPART (K)	280.8±0.5	285.9±0.4	286.1±0.4	283.7±1.0	284.4±0.7	282.3±0.7	288.0±0.7	284.3±1.1

RH at OMP (%)	NA	NA	26.8±3.1 *	36.0±0.0	31.2±0.9	6.6±0.3	9.50	17.5±6.4 *
RH from FLEXPART (%)	23.2±3.7	33.1±3.4	31.4±5.8	37.3±7.4	27.5±4.8	10.2±1.4	18.0±9.5	15.2±10.4
$T_{g,org}$ at site from meteorological data (K)	NA	NA	315.7 (296.4-344.5)	307.9 (291.6-332.9)	312.1 (294.7-338.6)	328.6 (310.2-356.9)	327.1 (308.9-354.9)	322.2 (300.5-353.8)
$T_{g,org}$ at site from FLEXPART data (K)	320.1 (317.8-322.4)	313.2 (310.5-315.9)	314.3 (309.8-318.8)	309.4 (303.4-315.4)	317.2 (314.1-320.4)	327.4 (326.7-328.1)	322.8 (316.7-328.8)	324.2 (317.7-330.8)

* Values are calculated using daily average since we do not have RH measurements during the sampling period.

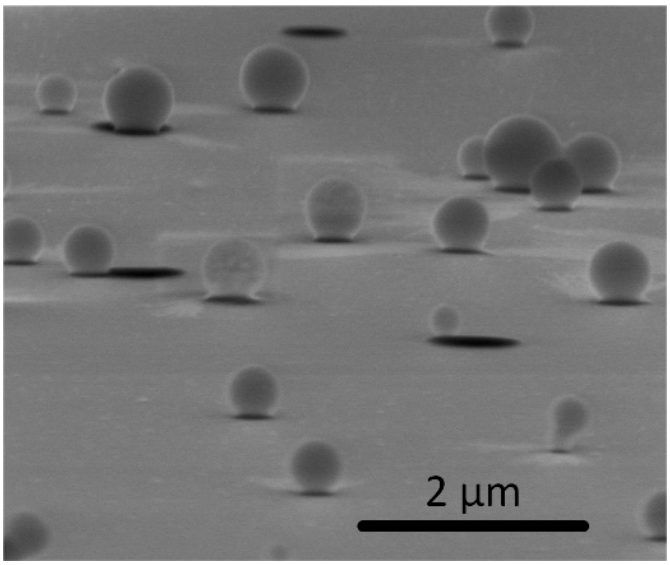

Figure S1. Representative tilted image of CNQX disodium salt particle generated from nebulizing 0.5 g L^{-1} aquatic solution.

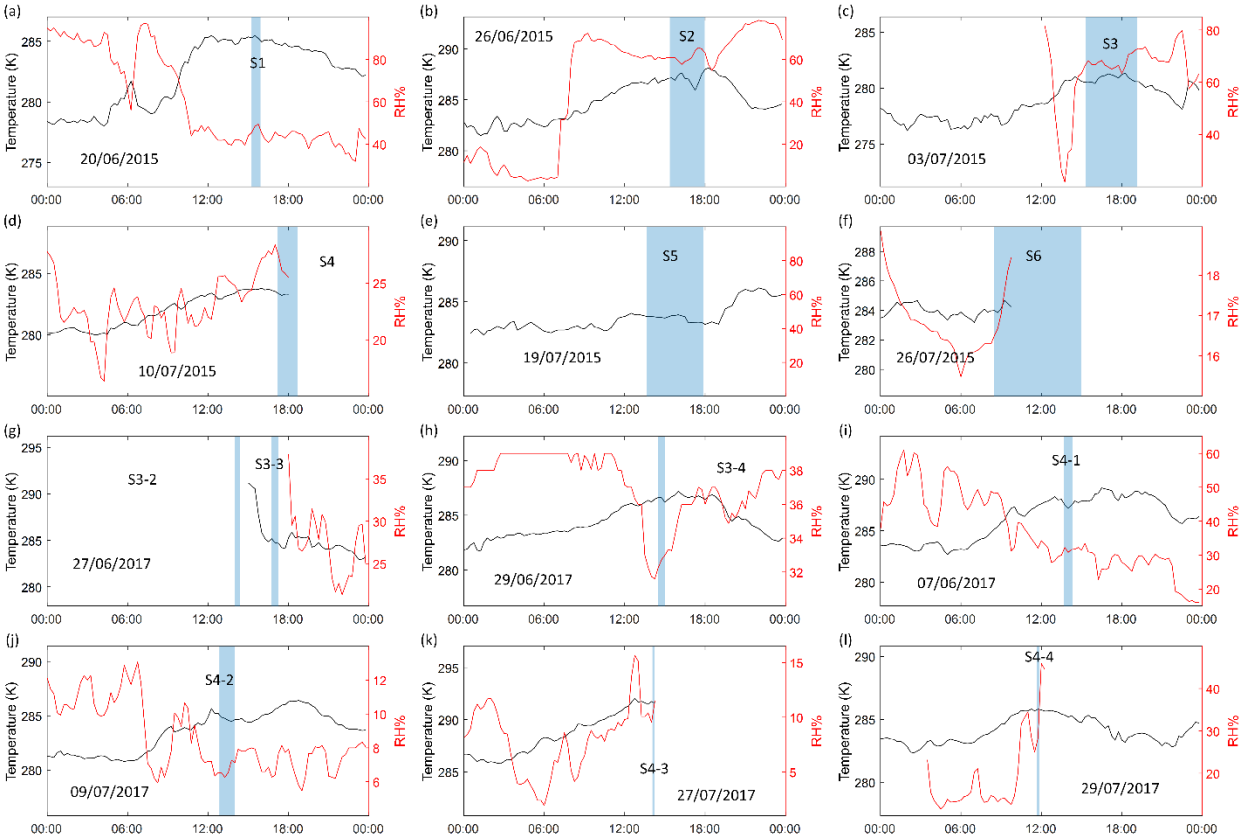

Figure S2. Hourly variation of temperature and relative humidity for available days. Shaded areas represent the sample collection periods.

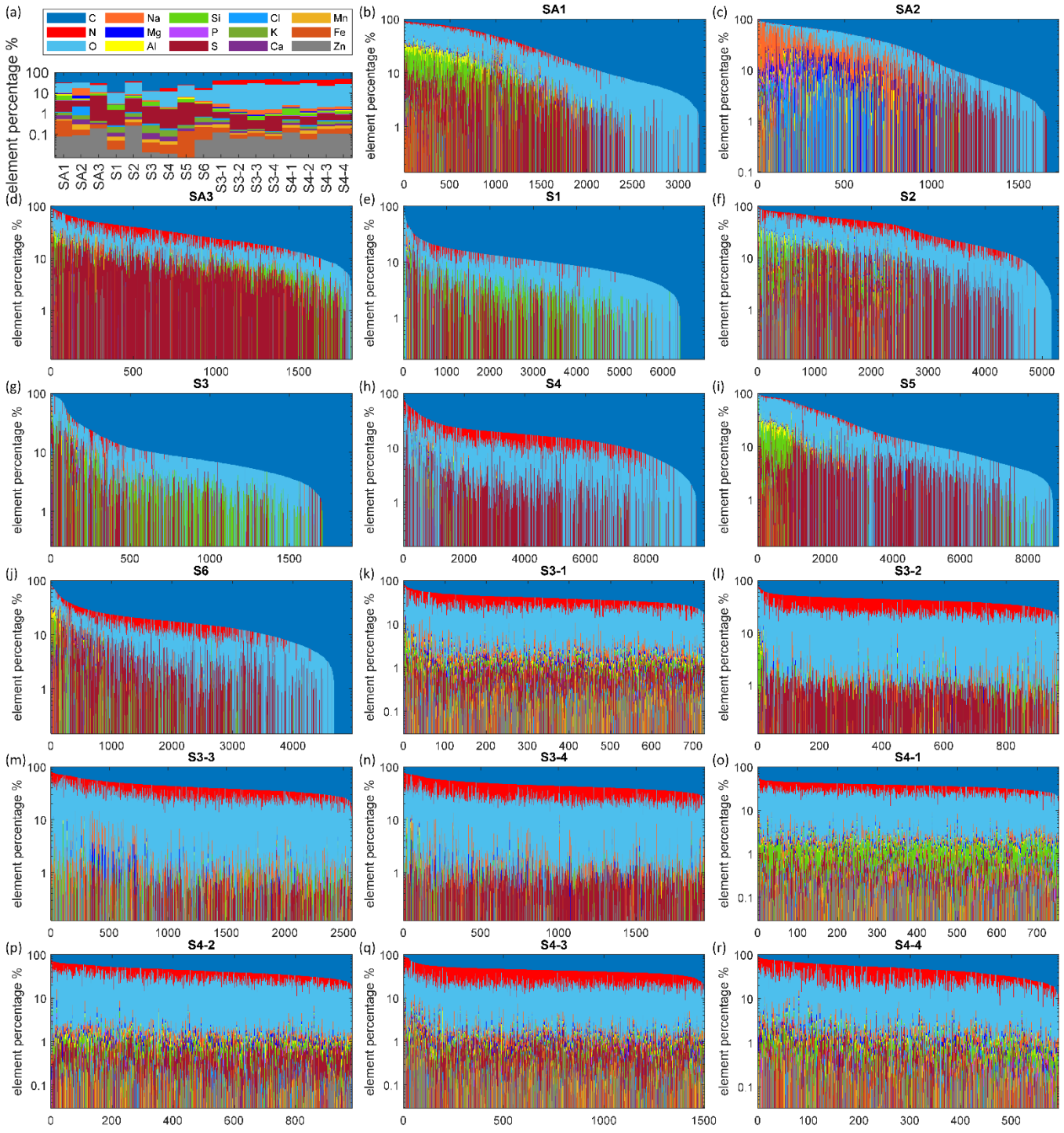

Figure S3. Relative element percentage of 15 elements (C, N, O, Na, Mg, Al, Si, P, S, Cl, K, Ca, Mn, Fe, Zn) for (a) average relative atomic ratios for all samples, (b) SA1, (c) SA2, (d) SA3, (e) S1, (f) S2, (g) S3, (h) S4, (i) S5, (j) S6, (k) S3-1, (l) S3-2, (m) S3-3, (n) S3-4, (o) S4-1, (p) S4-2, (q) S4-3, (r) S4-4. The X axis indicates the particle number.

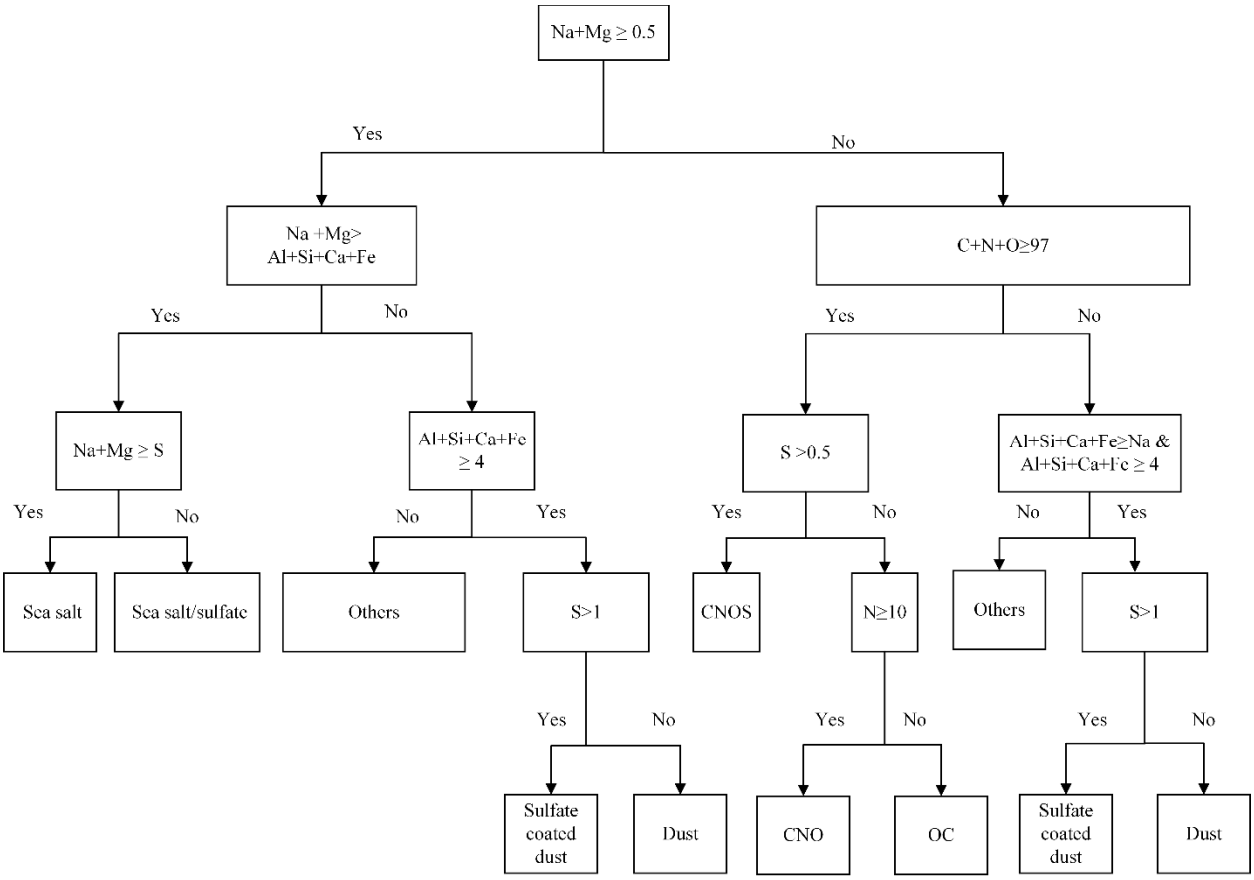

70

Figure S4. Flow chart to classify Pico 2017 particle types based on their element percentage retrieved from CCSEM/EDX measurements.

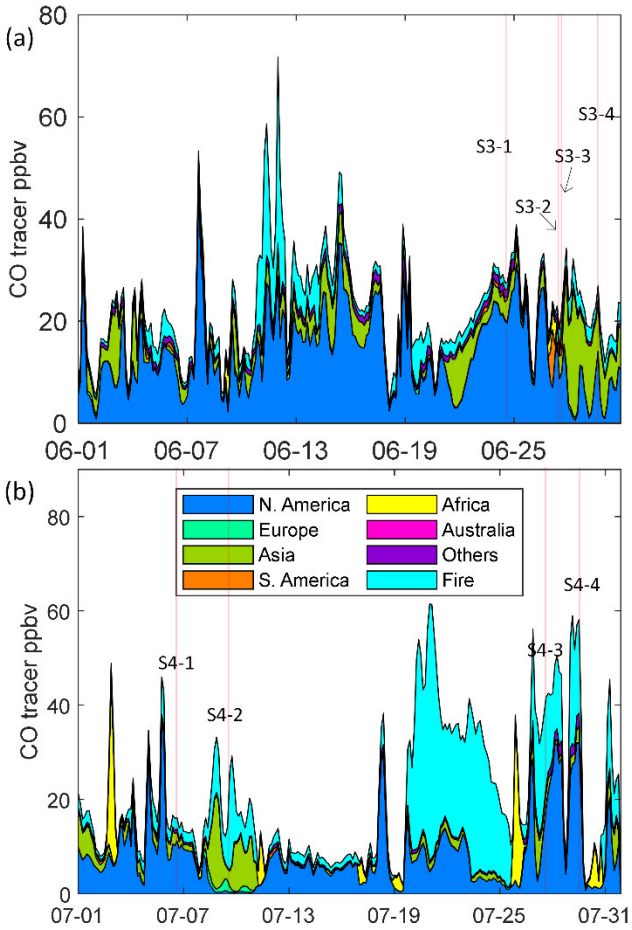

Figure S5. FLEXPART CO tracer simulation for (a) June 2017 and (b) July 2017.

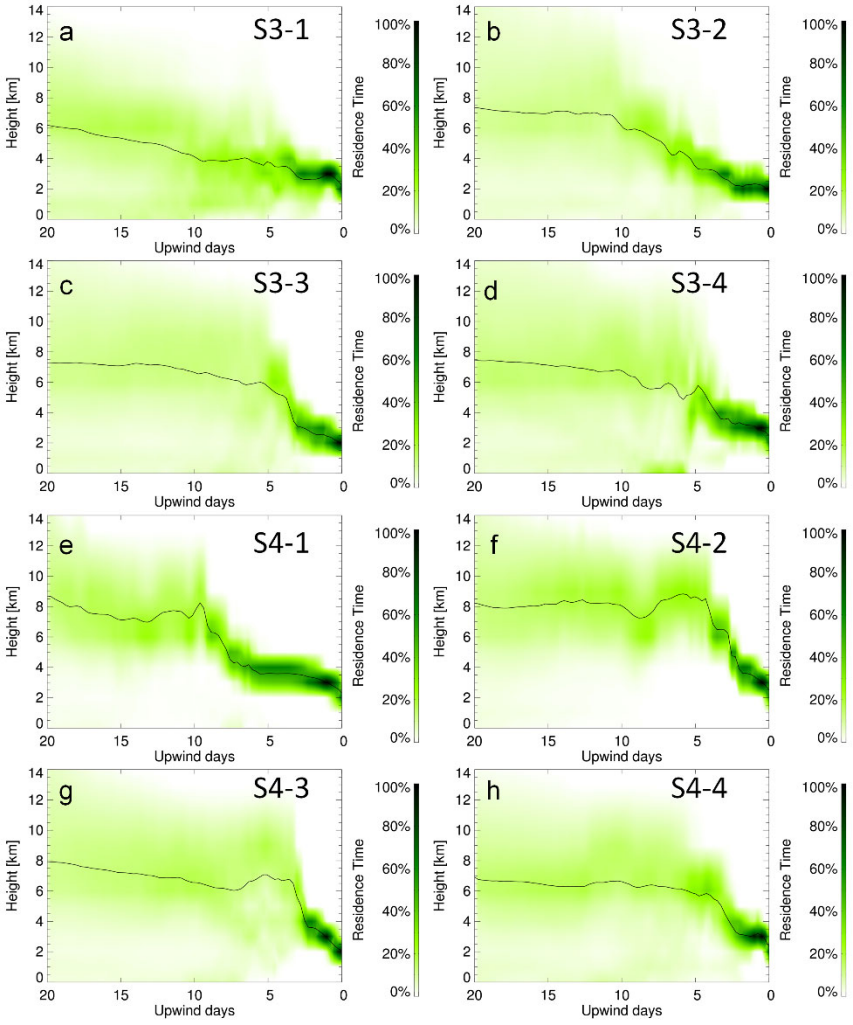

Figure S6. The vertical distribution of the retroplumes residence time at given upwind times retrieved from FLEXPART retroplumes for (a) S3-1, (b) S3-2, (c) S3-3, (d) S3-4, (e) S4-1, (f) S4-2, (g) S4-3, and (h) S4-4 for Pico 2017. The color bar represents the ratio of residence time to the highest residence time across the height scale at each upwind time. The black lines indicate the average height of the plumes during transport.

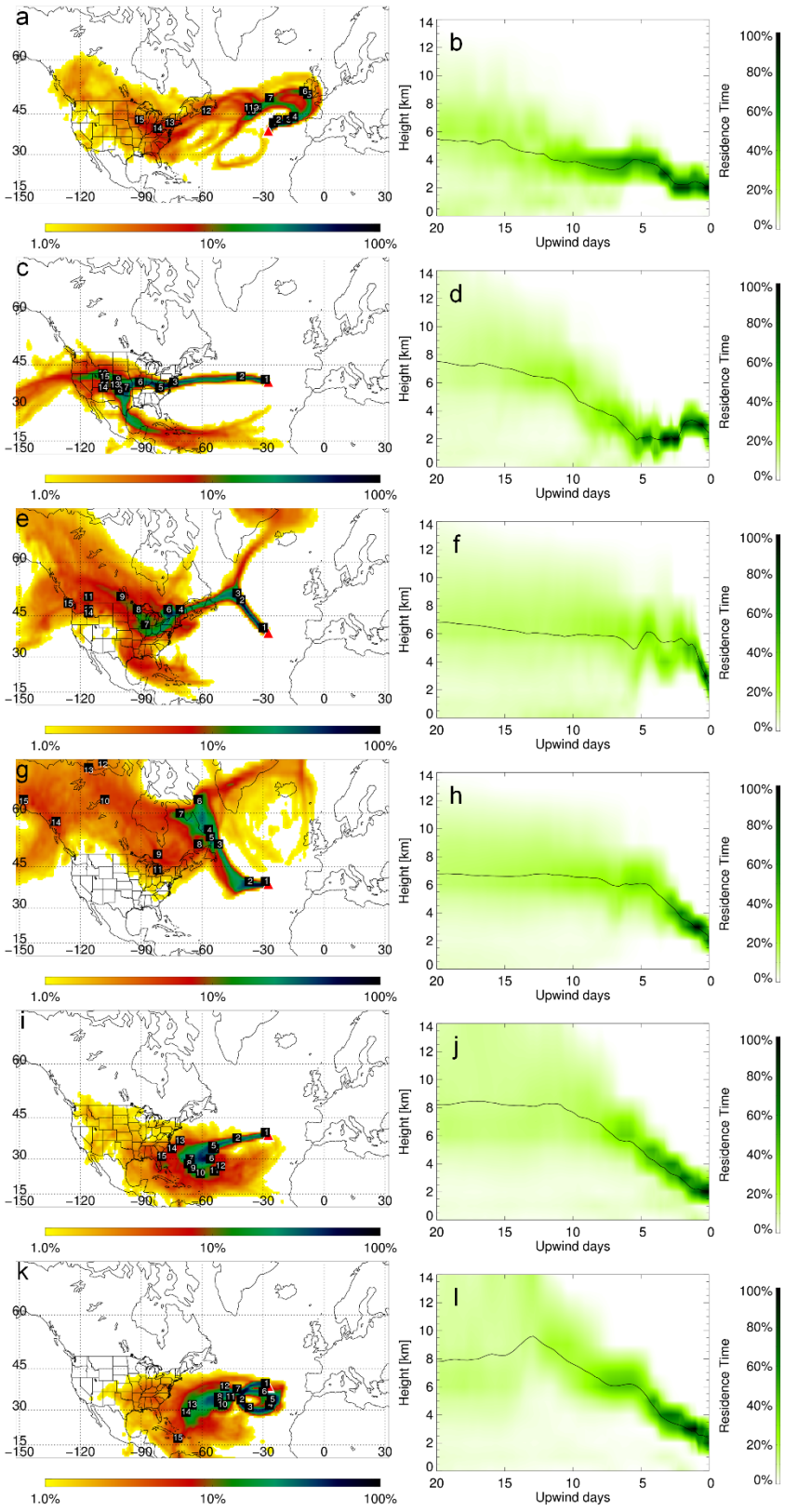

Figure S7. Column-integrated residence time over the 20-day transport time and the vertical distribution of the retroplumes residence time at given upwind times retrieved from FLEXPART retroplumes for Pico 2015.

(a, b) S1, (c, d) S2, (e, f) S3, (g, h) S4, (i, j) S5, (k, l) S6. For panels a, c, e, g, and i, the color bars indicate the ratio of column integrated residence time to the maximal residence time at each upwind time in the logarithmic scale, and the X-axis and y-axis represent latitude and longitude, respectively. For panels b, d, f, h, j, and l, the color bars represent the ratio of residence time to the highest residence time across the height scale at each upwind time, and the black lines indicate the average height of the plumes during transport.

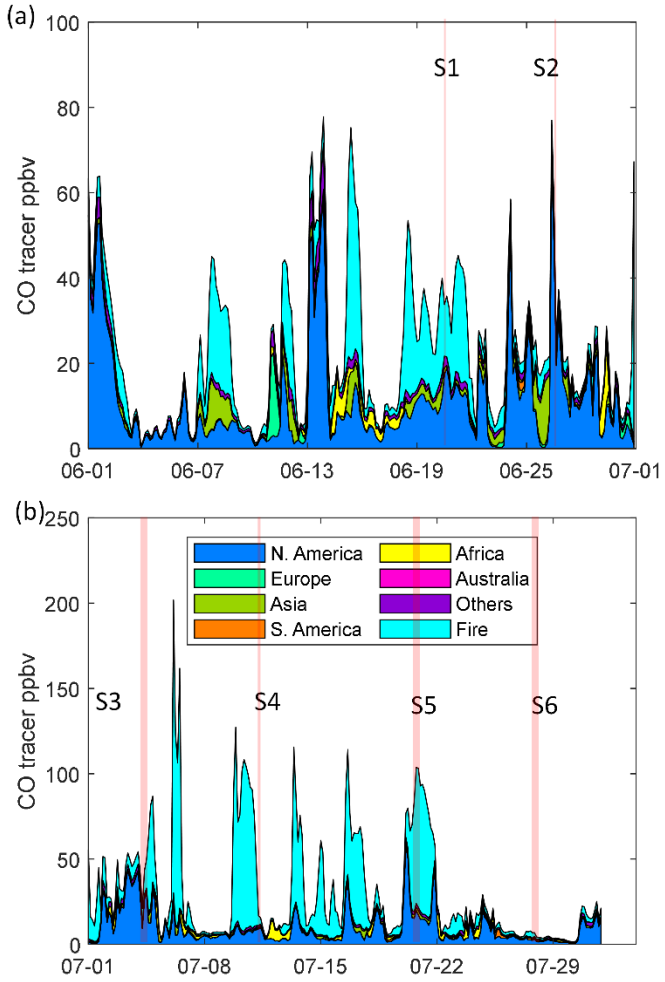

Figure S8. FLEXPART CO tracer simulation for (a) June 2015 and (b) July 2015.

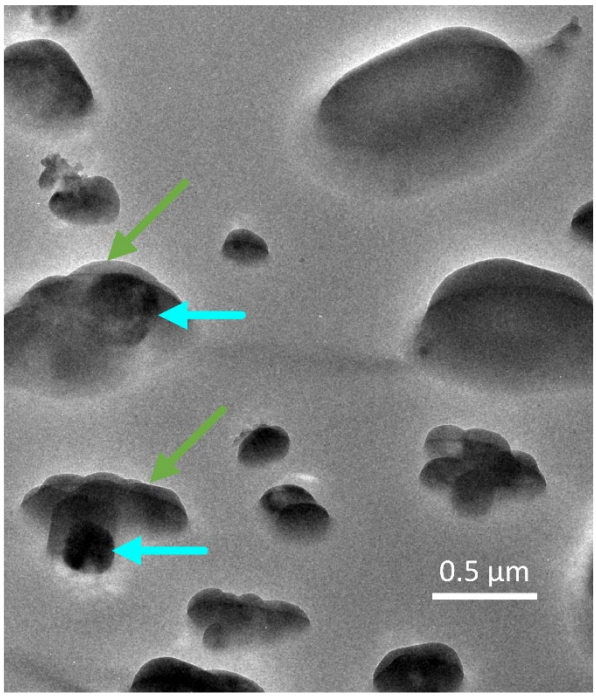

Figure S9. Representative tilted transmission electron microscopy (TEM) images (tilt angle 70°) for S3-2. Green arrows indicate examples of thin organic coatings, and cyan arrows indicate examples of internally mixed inorganic inclusions (e.g., sea salt, nitrate, sulfate, dust, cycled by solid red lines) coated by organics.

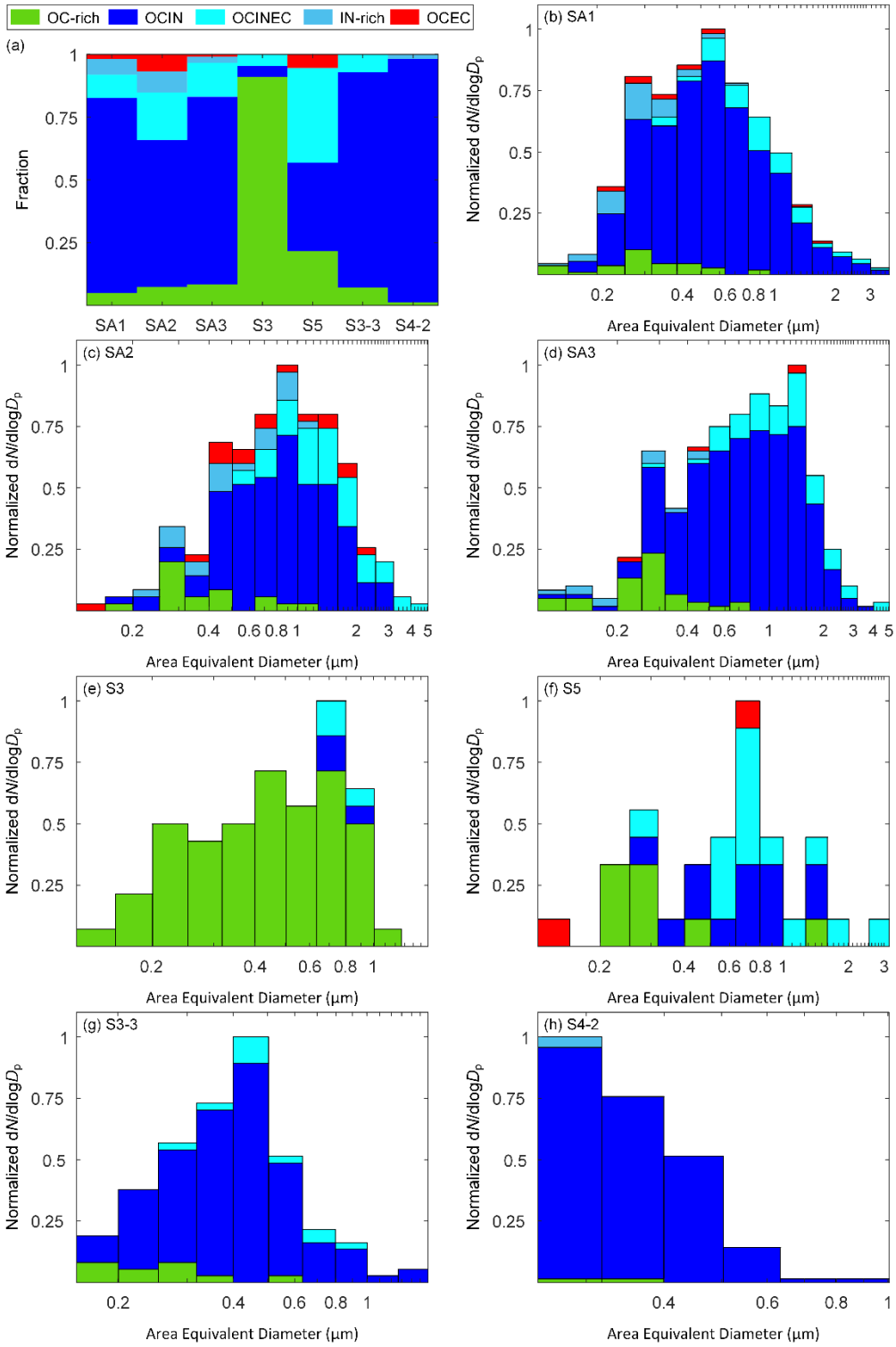

Figure S10. Chemically-resolved size distributions were inferred from the STXM-NEXAFS measurements for samples. (a) Fraction of different particle types for all samples, normalized chemically-resolved size distributions of (b) SA1, (c) SA2, (d) SA3, (e) S3, (f) S5, (g) S3-3, and (h) S4-2.

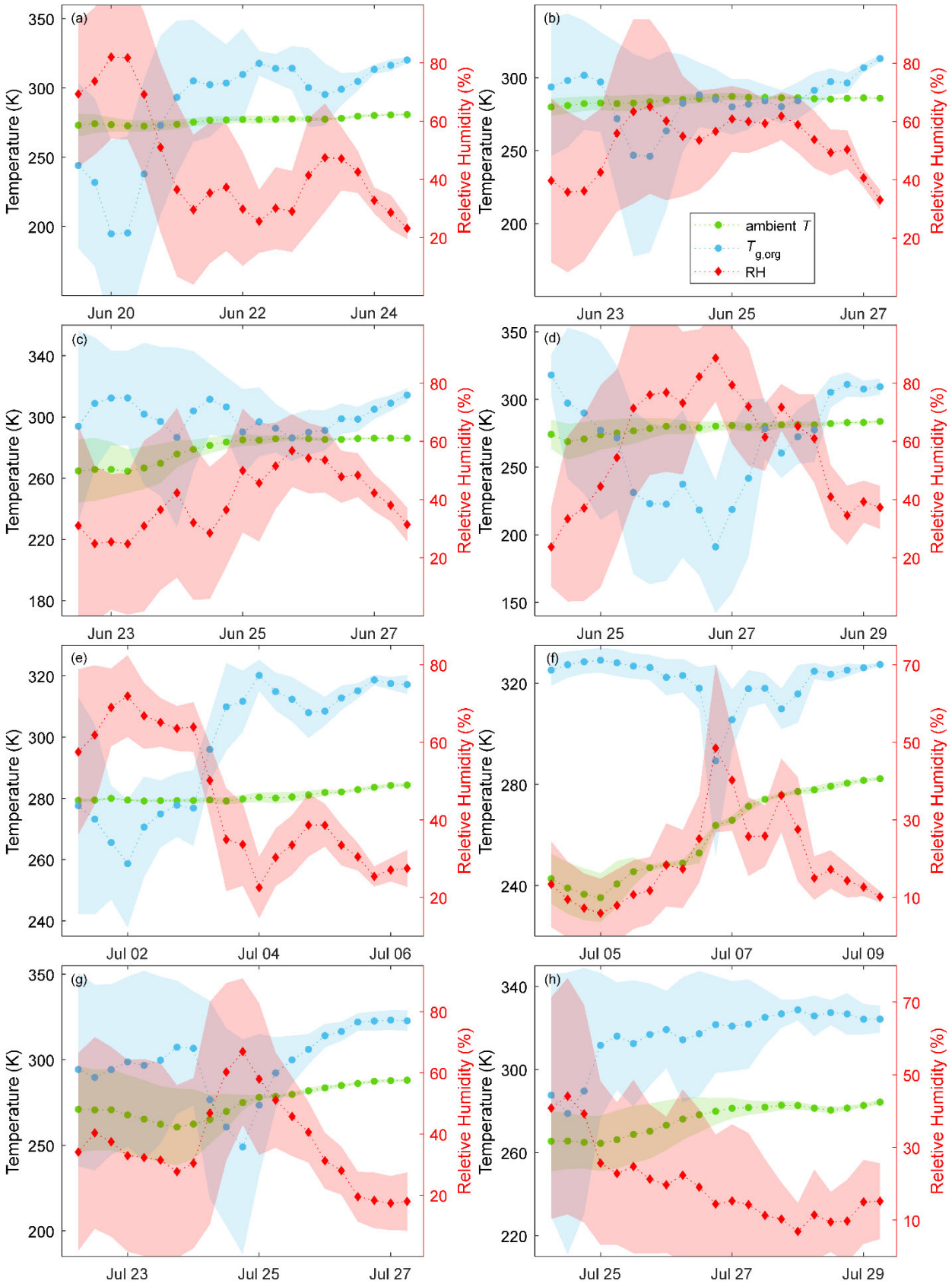
(a)
(b)
(c)
(d)
(e)
(f)
(g)
(h)
Temperature (K)
Reletive Humidity (%)
ambient T
$T_{g,org}$
RH
Jun 20
Jun 22
Jun 24
Jun 23
Jun 25
Jun 27
Jun 29
Jul 02
Jul 04
Jul 06
Jul 05
Jul 07
Jul 09
Jul 23
Jul 25
Jul 27
Jul 29

Figure S11. Mean ambient temperature (green) and relative humidity (RH) (red) extracted from the GFS analysis along the FLEXPART modeled path weighted by the residence time and the predicted RH-dependent $T_{g,org}$ values (blue) for (a) S3-1, (b) S3-2, (c) S3-3, (d) S3-4, (e) S4-1, (f) S3-2, (g) S4-3, and (h) S4-4. The blue and red shaded areas represent one standard deviation of ambient temperature and RH from the GFS analysis. The green shaded areas represent uncertainties of predicted $T_{g,org}$ estimated from the range of $T_{g,org}$(RH = 0%) and uncertainties in RH.

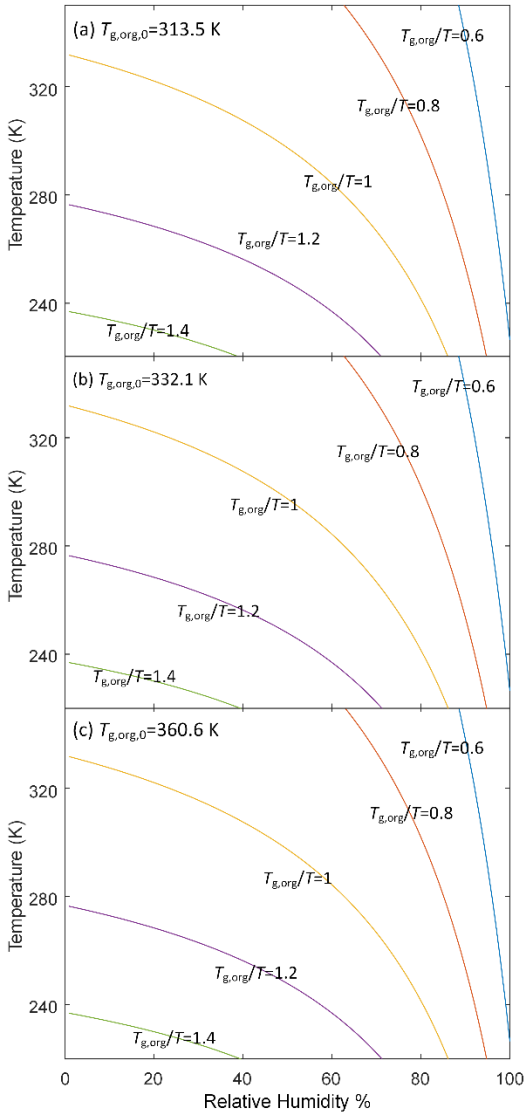

Figure S12. $T_{g,org}/T$ ratio as a function of temperature and relative humidity for organic particles transport in FT by using (a) minimum, (b) median, and (c) maximum dry glass transition temperatures of organics as reported in Schum et al., 2018 (313.5 K, 332.1 K, and 360.65 K, respectively).

References:

Kohl, I., Bachmann, L., Hallbrucker, A., Mayer, E. and Loerting, T.: Liquid-like relaxation in hyperquenched water at ≤ 140 K, PCCP, 7(17), 3210–3220, doi:10.1039/b507651j, 2005.

Schum, S. K., Zhang, B., Dzepina, K., Fialho, P., Mazzoleni, C. and Mazzoleni, L. R.: Molecular and physical characteristics of aerosol at a remote free troposphere site: Implications for atmospheric aging, Atmos. Chem. Phys., 18(19), 14017–14036, doi:10.5194/acp-18-14017-2018, 2018.

Shiraiwa, M., Li, Y., Tsimpidi, A. P., Karydis, V. A., Berkemeier, T., Pandis, S. N., Lelieveld, J., Koop, T. and Pöschl, U.: Global distribution of particle phase state in atmospheric secondary organic aerosols, Nat. Commun., 8, 15002, doi:10.1038/ncomms15002, 2017.

Wang, B., Lambe, A. T., Massoli, P., Onasch, T. B., Davidovits, P., Worsnop, D. R. and Knopf, D. A.: The deposition ice nucleation and immersion freezing potential of amorphous secondary organic aerosol: Pathways for ice and mixed-phase cloud formation, J. Geophys. Res., 117(16), D16209, doi:10.1029/2012JD018063, 2012.